Title: Evaluation of parameters governing dark and photorepair in UVC-irradiated *Escherichia coli*

Authors:

Mostafa Maghsoodi[1], Grace L. Lowry[1], Ian M. Smith[1], Samuel D. Snow[1*]

[1]Department of Civil and Environmental Engineering, Louisiana State University, 3255 Patrick Taylor Hall, Baton Rouge, Louisiana 70803, United States.

*Corresponding author: ssnow@lsu.edu;

Abstract:

After decades of UV disinfection practice and numerous studies on the potential for pathogens to undergo dark or photo-repair after UV exposure, recent advances in UV light emitting diode (LED) technologies prompt renewed attention to bacterial reactivation and regrowth processes after UV exposure. The aspect of photorepair conditions warrants particular attention, because even studies on conventional mercury vapor lamps have not sufficiently characterized these parameters. Wastewater encounters a wide range of environmental conditions upon discharge (e.g., solar irradiation and dissolved organics) which may affect repair processes and ultimately lead to overestimations of pathogen removal. *Escherichia coli* was used here to investigate the impacts of changing reactivation conditions after UV_{254} and UV_{278} irradiation. UV_{254} and UV_{278} doses of 13.75±0.4 $mJ \cdot cm^{-2}$ and 28.3±0.8 $mJ \cdot cm^{-2}$ were required to induce a 3.0-log inactivation of *E. coli*, respectively. Specifically, photoreactivation conditions were varied across dissolved organic matter (DOM) content and photoreactivation wavelengths and intensities. Photoreactivation achieved higher log recoveries than dark repair, ranging from 0.8 to 1.8 log differences, but a secondary disinfection effect occurred under UVA irradiation. During photoreactivation, humic acid inhibited the initial repair of UV_{278}-dosed *E. coli* but culture media enhanced recovery for both dosage wavelengths. Photoreactivation profiles under

UV_{395}, UV_{365}, and visible light depended on both fluence and time, with more regrowth observed upon exposure to visible light and the least under 365 nm. The susceptibility of *E. coli* to UVA was increased by prior exposure to UVC.

Keywords:
UV Disinfection; bacteria; photoreactivation; photorepair; regrowth; UV LEDs

1. Introduction

Across the globe, microbial contaminants in wastewater discharges threaten public health with water-borne diseases.(1, 2) For this reason, it is essential that disinfection technologies in water treatment systems effectively inactivate pathogens. Conventional ultraviolet (UV) dosing systems are known to be effective at inactivating pathogens via DNA damage,(3) yet there is an important caveat: the potential for cellular repair mechanisms to reactivate UV-dosed organisms.(3, 4) Currently, nearly all germicidal UV (or UVC, 200 to 280 nm) driven inactivation processes use either low pressure mercury lamps with a nearly monochromatic emission at 254 nm or medium pressure lamps with a polychromatic emission.(5, 6) Recent innovations in LED technologies will make it possible to replace mercury lamps with LED counterparts in many UV dosing applications.(5, 7) UV LEDs will ultimately offer several improvements over Hg lamps; for example, UV LEDs provide the ability to optimize wavelengths, reduce light attenuation (via redshifted wavelengths and innovative contactor designs), reduce operational costs, and have longer life expectancies.(8) As challenges of production cost and power output are resolved, UVC LEDs are expected to transform the UV disinfection industry.(9, 10) It is anticipated that UV LEDs will follow the same cost and efficiency trajectory that was observed for other type of LEDs. As an example, the wall plug efficiencies (the optical power output divided by the electrical input power) of blue and red

LEDs were increased 80% and 60% respectively in 2010.(11) The American National Standards Institute (ANSI) revised its rule for ultraviolet microbiological water treatment systems (55-2019) in November 2019 to include germicidal LEDs in its guidance.(12)

Despite the damage caused by UV irradiation, many microorganisms can counteract the defects with repair mechanisms.(13) Bacteria have two cellular repair modes: dark repair and photoreactivation. Dark repair occurs in the absence of light and replaces damaged DNA sites with undamaged nucleotides via two pathways: base excision repair and nucleotide excision repair.(14) Dark repair mechanisms are controlled by the expression of the recA gene which regulates the induction of over 20 genes.(15) The recA protein plays both direct and indirect roles in recombinational repair and controls the induction of the SOS repair genes through its protease function.(16) The dark process is only able to remove thymine dimers when glucose is present.(17) Photoreactivation is a process by which bacteria or bacteriophages (via host cells) can recover from induced UV damage upon exposure to visible or UVA (~320 to 400 nm) light.(18, 19) In this process, the pyrimidine dimer photoproducts created by UVC or UVB exposure are repaired by photoactivated enzymes.(19, 20) Photolyase is the biomolecule primarily responsible for the photoreactivation process, containing monomeric proteins of 450-550 amino acids and two non-covalently bound chromophore cofactors.(21) Photolyase is activated by the energy of photons with wavelengths from 330 to 480 nm,(22) binds to cyclobutane pyrimidine dimers (CPDs) or pyrimidine-pyrimidone photoproducts (6-4 PPs), and initiates cycloreversion of the cyclobutane ring, mitigating the adverse effect of UV irradiation.(22)

Several predictive models have been put forward since the discovery of photoreactivation with the aim to better understand the fate of UVC-dosed bacteria in environmental systems.(23-25) Building from early models, Nebot Sanz et al. (2007) incorporated an induction period, a lag interval between initial reactivation light exposure and observed reactivation, and accurately

matched their experimental data. In Nebot Sanz's model, the data for photoreactivation were obtained across several experimental dimensions, including microbe type, reactivation light exposure, and dark repair time, but their work only considered a low dose of reactivation light (0.1 mW/cm^2 of UV_{360} for 4 h), well below typical solar intensities (monthly average of 1.0 mW/cm^2 for hourly solar radiation in the range of 290 nm to 385 nm).(26) This model was later revised in 2012 by Velez-Colmenares and coworkers by considering the effects of sunlight during reactivation, introducing a first order decay term to their predictive model for cell survivability.(27) In 2017, Li et al. published another adaptation of the Nebot Sanz 2007 model when comparing inactivation by UV LEDs and mercury lamps; their study also used a low photoreactivation dose of 0.12 mW/cm^2 over 8 h. In all these reports, none considered the reactivation light intensity as a variable; most studies examined photorepair on the basis of irradiation time, not fluence.

Bacterial repair dynamics may be influenced by the type of damage inflicted, so it is important to determine whether novel UVC dosing wavelengths cause differential repair outcomes. Photoinduced cellular damage can occur in a variety of ways. UVC photons can directly photolyze protein chromophores and cause generalized oxidative stress.(28) Similarly, UVB can cause direct or indirect (via production of endogenous reactive oxygen species) damage to cellular components.(29) The predominant mechanism of UVC inactivation of microorganisms is by causing specific damage to DNA or RNA.(30) In this process the light causes two predominant types of lesions in the genetic code: CPDs and 6-4 PPs.(19, 31) Other nucleic acid photoproducts, such as Dewar isomers, pyrimidine hydrate, thymine glycols, and dipurine adducts, are also produced in smaller amounts during UV irradiation.(13, 14) The type of damage induced depends, in part, on wavelength; for example, in the UVC range (200 to 280 nm) the predominant lesions are CPDs and 6-4 PPs and in the UVB range (280 to 320 nm) the formation of Dewar isomers is more efficient and sometimes they are the second most frequent

photoproducts after CPDs.(14, 32) In this way, adapting a UV_{254} dosing system to a UV_{278} source may change the nature of the damage microorganisms receive.

When wastewater effluent discharges into natural waters, the presence of dissolved organic matter (DOM) and the average incident solar irradiation, about 5% of which is in the UV spectrum,(33) become important considerations. DOM can impact the activity of microbes by directly providing substrate (assimilable organic carbon) for regrowth after repair,(34) by promoting the uptake of nutrients, or—in some cases—by inhibiting growth via toxic effects.(35) The impact of DOM on recovery processes after UVC exposure, however, is not well understood. Likewise, upon mixing with a receiving water, irradiated microorganisms from an effluent discharge will be transported to different positions in the water column and receive differing amounts of solar irradiation. At present, few data are available on photoreactivation under variable reactivation light conditions.

In this work, the implications of variable reactivation conditions are explored in the context of using different germicidal wavelengths for *E. coli* disinfection. The extent and kinetics of reactivation are assessed during dark- and photorepair across DOM types and quantities. Photoreactivation profiles for different reactivation light intensities and wavelengths are analyzed on fluence and time bases.

2. Materials and methods

2.1. Chemicals

Humic acid and Potassium trioxalatoferrate (III) trihydrate were obtained from Alfa Aesar (Haverhill, MA). 1,10-Phenanthroline, sodium acetate anhydrous, sulfuric acid, Tryptone, Yeast Extract, Dextrose, NaCl, $CaCl_2$, $MgSO_4$ and Phosphate Buffered Saline (PBS) were obtained from VWR (Radnor, PA). Ultrapure water (>18.2 MΩ-cm) from a Nanopure Infinity system (Thermo Fisher Scientific Inc., Waltham, MA) was used.

2.2. Culturing and Enumeration

E. coli was used in this work because *E. coli* has been used as an indicator microbe for confirming the presence of pathogens.(36) *E. coli* (ATCC® 15597™) was obtained from American Type Culture Collection (ATCC, Manassas, VA). To enumerate *E. coli*, samples were serially diluted, and the concentration of each sample was measured via a spread plate colony counting technique. In this technique, a sample aliquot was spread on nutrient agar plates then incubated at 37°C for 24 h. Agar plates and culture broth (CB) media contained tryptone, yeast extract, dextrose, NaCl, $CaCl_2$, and $MgSO_4$.(37) *E. coli* sample processing was performed in phosphate buffered saline (PBS) containing 137 mM NaCl, 2.7 mM KCl, and 9.5 mM Phosphate buffer with the resulting pH between 6.6 to 7.2. All samples were measured with at least three plates per sample point and experiments were performed in at least triplicate; error bars represent the standard error of these measurements.

2.3. Irradiance Measurement

The irradiances of each light source were measured by BLUE-Wave UVNb-25 Spectrometer (StellarNet Inc., Tampa, FL). The lamp emission spectra were also recorded. The Bolton and Linden (2003) method was used to calculate UV fluences with the units of $mJ \cdot cm^{-2}$ to account for water, Petri, reflectance, divergence, and attenuation factors.(38) These calculations treated the LEDs to be monochromatic for the purpose of reporting irradiance, since the spectrometer provided a wavelength-integrated measurement. To complement the radiometric fluence calculations, chemical actinometry experiments were performed to measure the intensity of light in units of einstein/min. Potassium trioxalatoferrate (III) trihydrate was used as an actinometer. All the actinometric experiments were performed in a dark room to eliminate the effect of the ambient light. Samples containing potassium trioxalatoferrate (III) trihydrate, sodium acetate and sulfuric acid were irradiated with different light sources and were then mixed with 2 ml of 0.2% aqueous solution of 1,10-phenanthroline and after diluting the mixture

with DI water to 10 ml, the absorbance of samples was measured at 510 nm.(39) Equation (1) was used to calculate the light intensity (I):

$$I = \frac{AV_2V_3}{\varepsilon d \emptyset_\lambda t V_1} \quad (1),$$

where the unit for intensity is einsteins/min. V_1, V_2, and V_3 correspond to the volume of the sample taken from the batch, the total volume of actinometer solution, and the dilution volume, respectively, *t* is the irradiation time, and *d* is the cell path length used to measure absorption (A). An extinction coefficient (ε) value of 1.11×10^4 L $mol^{-1} \cdot cm^{-1}$ for the ferrous 1,10-phenanthroline complex was used based on Halchard and Parker's work, and quantum yield values at given wavelengths (ϕ_λ) of ferrous production were obtained from a previous report.(39)

2.4. UV Inactivation

Inactivation experiments were performed by exposing *E. coli* to UV light from several sources. A UV LED (LG Innotek UVC 6868, South Korea) with an emission peak at 278 nm (UV_{278}, 11.5 nm FWHM) was used, and quasi-collimated irradiation was achieved by situating the LED above a black tube with the sample below; a schematic of this cabinet is shown in Figure S1 of the Supporting Information (SI). Separately, a 15 W low pressure mercury lamp (Sankyo Denki Co., Japan) with an emission peak at 254 nm (UV_{254}, 4.0 nm FWHM) was used. All emission spectra from light sources used for their germicidal effects are illustrated in Figure 1. All inactivation experiments were conducted inside an enclosed photoreactor cabinet equipped with a magnetic stirrer and kept at room temperature via cooling fans. The distance between samples and UV light source was adjusted to 20 cm which provided intensity values of 371 $\mu W \cdot cm^{-2}$ for the Hg lamp and 722 $\mu W \cdot cm^{-2}$ for the UV LED.

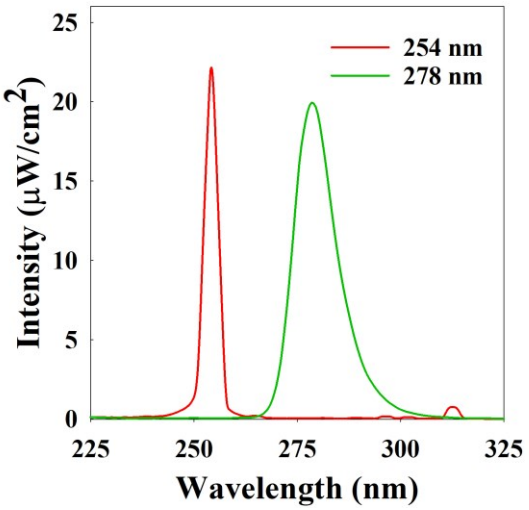

Figure 1. Emission spectra from UVC lamps used for disinfection.

UV dosing was performed in a sterilized glass Petri dish with a 5 cm diameter and a depth of 1.5 cm; *E. coli* was diluted by adding PBS to reach a reactor volume of 10 mL. The resulting concentration was 10^7 CFU·mL^{-1} for *E. coli*. DOM experiments were performed using either 25 mg·L^{-1} humic acid (HA) or CB at a dextrose concentration of 25 mg·L^{-1}. The absorbance of each sample was measured in a 1 cm quartz cuvette using a UV-Vis spectrophotometer (UV3100-PC, VWR, USA).

2.5. Repair Experiments

Repair experiments were conducted for 9 h periods under dark or irradiated conditions after imposing at least a 3.0-log inactivation to be consistent with similar, recent work.(36) In these cases, N_o was defined as the number of viable cells per volume in solution prior to disinfection; N_d was used to designate the viable cells at the end of disinfection and the beginning of repair; and N denotes the concentration at a given time. Sample aliquots were taken at intervals, serially diluted, and plated immediately thereafter. In dark repair experiments, samples were kept in a clean dark chamber for 9 h. Five different light conditions including UVA lights with emission peaks at 365 and 395 nm and a visible light (see Figure 2 for obtained emission spectra) were

used to investigate fluence and wavelength effects on the photoreactivation process;

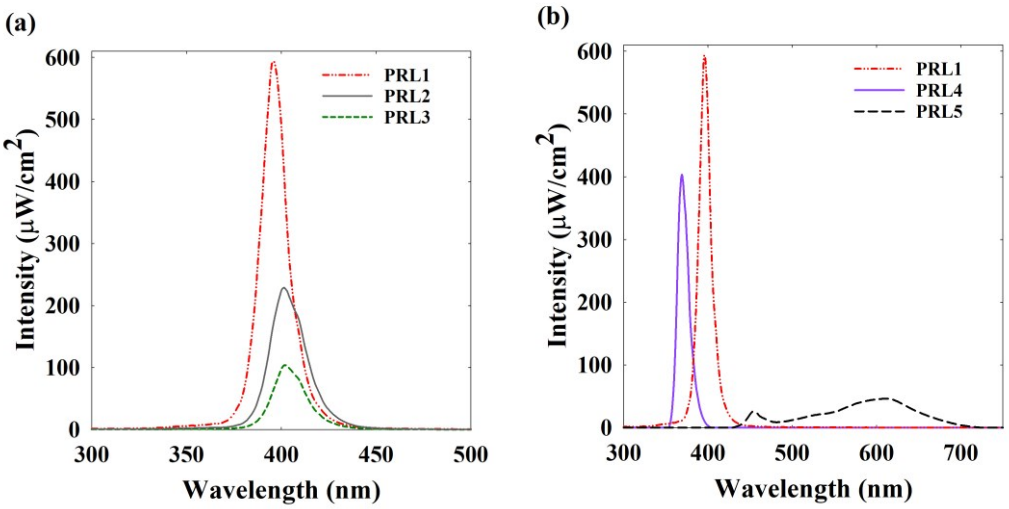

Figure 2. Emission spectra of lamps used for experiments with variable photoreactivation (a) intensities and (b) wavelengths.

abbreviations, emission parameters, and manufacturer information are provided in Table 1. PRL refers to photoreactivation lamp and the numbers are arbitrarily assigned such that PRLs 1-3 are UV_{395} lamps of differing intensities, PRL4 is a UV_{365} lamp, and PRL5 is a polychromatic white lamp. The majority of the photoreactivation experiments were conducted using PRL1. The effects of irradiation dosages on photoreactivation were assessed using three LED arrangements with emissions centered at 395 nm: PRL1, PRL2, and PRL3. The effects of wavelength on photoreactivation were investigated using three lamps: PRL1, PRL4, and PRL5. The visible light case (PRL5) adds a case relevant to conditions with limited UV light, such as indoor storage of UV-treated drinking water. The effects of DOM on the repair processes were assessed by adding 25 $mg \cdot L^{-1}$ of DOM (either HA or CB) to the reaction mixture prior to the UV inactivation step. Data are presented primarily as normalized log values ($\log[N/N_d]$) to compare the repair of different experiments on a basis of relative recoveries. The slopes of the decay portion of photoreactivation experiments were compared via a t-test to determine if the difference in the results of experiments is significant ($p < 0.05$). Survival fractions (S_t, N/N_o*100) are used when evaluating predictive models.

Table 1. Actinometry data for light sources used in photoreactivation experiments.

Abbreviation	Light intensity (einsteins/min)	Emission peak (nm)	LED manufacturer	FWHM (nm)
PRL1	8.04×10^{-5}	395	LG Innotek Co., 6868	15.5
PRL2	2.19×10^{-5}	395	TSLC Corp., C3535U-UNL	15.5
PRL3	7.33×10^{-6}	395	TSLC Corp., C3535U-UNL	15.5
PRL4	9.38×10^{-5}	365	LG Innotek Co., 6868	15.1
PRL5	6.49×10^{-7}	Polychromatic, visible 3000K	Brizled Inc., DDL6	N/A

2.6. Photoreactivation Model and Parameterization

A model put forward by Velez-Colmenares et al. in 2012, which included a decay term was used to fit experimental data and to compare how prior estimations of model parameters map onto present observations. The Velez-Colmenares model (VC model hereafter) shown in Equation 2 was derived to incorporate a photorepair term with a decay term for the germicidal effects of sunlight. In the equation,

$$S_t = (S_m \cdot e^{-M_s t}) - (S_m - S_o) \cdot e^{-(k_s + M_s)\cdot t} \quad (2),$$

S_t is survival at time t (min), S_m is the maximum survival ratio, S_o is the initial survival fraction immediately after UVC irradiation, $(S_m - S_o)$ is thus the fraction of microorganisms that can be reactivated with respect to the initial concentration, M_s represents the rate constant for UVA decay (min^{-1}), and k_s is the photoreactivation rate constant (min^{-1}). Predictive model fits were generated via Microsoft Excel spreadsheets using parameters derived from either the UVC-fluence empirical relationships put forward alongside the VC model or by using the Excel Solver functionality.(27) In the Solver analysis, the squared sum of errors value was minimized for the difference between predicted and observed values while constraining the M_s term to be $\geq$ observed decay rates, discussed below, and the $(S_m - S_o)$ term to be the difference between the solver formulation for S_m and the observed S_o value. R^2 values were determined according to the total variance between observed data and model fit.

3. Results

3.1. *E. coli* inactivation

Inactivation profiles of *E. coli* by different wavelengths in the presence and absence of DOM are shown in Figure 3. In the absence of DOM, the UV doses, reported as incident intensities, required to obtain 3.0-log inactivation at 254 nm and 278 nm were found to be 13.75 mJ·cm^{-2} and 28.3 mJ·cm^{-2}, respectively. The UV_{254} dose requirement of 13.75 mJ·cm^{-2} was similar to the 12 mJ·cm^{-2} in a 2017 study;(40) the UV_{278} dose of 28.3 mJ·cm^{-2}, however, was surprising because most reports place the dose requirement for a 3-log reduction near 12 mJ·cm^{-2}.(36, 40) The discrepancy here appears to relate to the extended shoulder, observed to extend to about 12 mJ·cm^{-2}. In the presence of DOM, the required doses for obtaining 3.0-log inactivation, after adjusting for light absorption, did not appear to be significantly different from the non-DOM cases, at 11.6 mJ·cm^{-2} for UV_{254} and 26.6 mJ·cm^{-2} for UV_{278}. At higher concentrations (50 mg·L^{-1}), humic substances have been shown to provide localized UV shielding for bacteria, beyond attenuation in the bulk phase.(41) The 25 mg·L^{-1} used here did not appear to significantly affect the disinfection process.

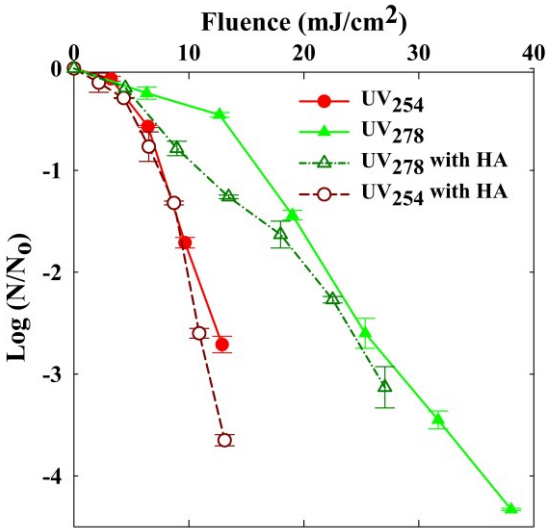

Figure 3. Inactivation of *E. coli* with 25 mg·L^{-1} HA or in PBS alone by UV_{254} and UV_{278}.

3.2. Dark repair of *E. coli*

Dark repair experiments were conducted using bacteria inactivated by UV_{254} or UV_{278}, with results plotted in Figure 4. A reference line shows the typical growth kinetics of *E. coli* over 9 h in the dark; the trendline was calculated from experiments shown in Figure S2 in which *E. coli* was diluted by 3-log, in place of disinfection, then provided HA, CB, or just PBS. After 9 h, *E. coli* recovered 1.3 and 1.1 logs after UV_{254} or UV_{278} exposure, respectively. These values fell well below the growth of *E. coli* that were not subject to UVC dosing, but the initial recovery of cells exposed to UV_{278} was more rapid than growth alone, when DOM was available. The presence of a carbon source, HA or CB, allowed UV_{278}-exposed cells to repair faster than all other cases. Here, dark repair rates, between 0.5 and 1.6 logs, outpaced total dark recoveries reported by Nyangaresi et al. (2018), which were at most 0.24 logs for several disinfection wavelengths. Given the minimal difference between irradiation sources with peaks at 275 and 278 nm and that both studies accounted for inactivation on a fluence basis, the difference in recoveries is likely a result of differing solution conditions: Nyangaresi et al. used deionized water for all their experiments while PBS was used here to avoid cell death via osmotic shock.

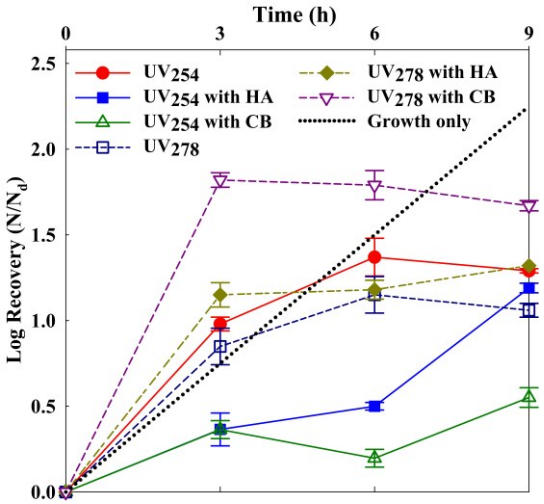

Figure 4. Dark repair of UV_{254}- or UV_{278}-dosed *E. coli* with 25 mg·L^{-1} HA, 25 mg·L^{-1} CB, or in PBS only. The black dotted line (••••) represents the growth of *E. coli* after dilution, in place of UV exposure, to the same initial concentration.

The effects of DOM on dark repair were investigated by adding HA or CB to the reaction solutions. HA has been shown to behave as a growth regulator for some bacteria and may affect cellular repair processes.(42) Most dark repair observations here matched the profile of the reactivation model put forward by Nebot Sanz et al. (2007) with an induction period, growth phase, stabilization phase and decay period. HA inhibited the recovery of UV_{254}-dosed *E. coli* in the first 6 h, but the rate increased between 6 and 9 h such that the log recovery with HA at 9 h was similar with or without HA. The recovery was higher in the absence of HA for the first 6 h of dark repair after UV_{254} exposure than with HA; this trend was not observed in the dark repair profile of UV_{278}-dosed *E. coli*. CB was used to provide *E. coli* with favorable growth conditions, in order to investigate the effect of nutrients on the dark repair. Although more recovery was expected with CB because of the availability of glucose, a highly efficient carbon and energy source for *E. coli*,(43) fewer UV_{254}-dosed bacteria recovered in the presence of CB than without any DOM. After UV_{278}-dosing, however, more repair was observed with added CB than without. CPD and 6-4 PP are formed at higher rates during irradiation by UV_{254} than by UV_{278},(44) whereas red-shifted wavelengths have been found to promote more oxidative stress.(45) Given that photolyase functions specifically to repair nucleic acid dimerizations, it is likely that the oxidative damage is more difficult for bacteria to repair.

3.3. Photoreactivation of *E. coli*

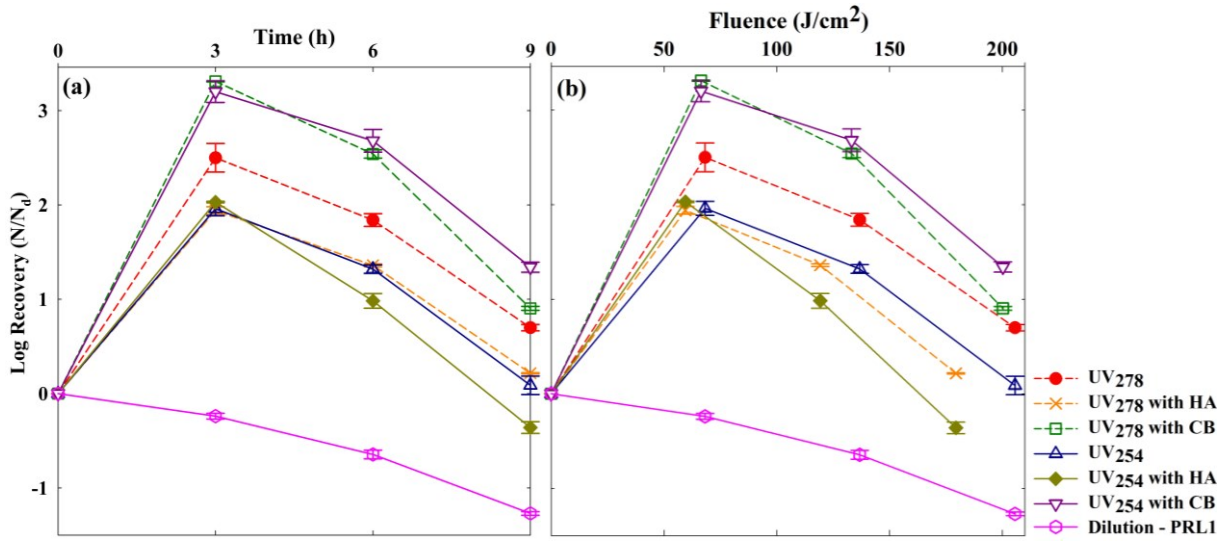

Figure 5. Photoreactivation of *E. coli* using PRL1 in the presence or absence of 25 mg·L^{-1} of HA or CB after inactivation by UV_{254} and UV_{278}. Data are displayed on the bases of (a) time and (b) fluence. A reference of *E. coli* inactivation under PRL1 with no prior UVC-dosing is also shown (—○—).

The photoreactivation of *E. coli* after different UVC sources was studied using PRL1 (with an emission peak at 395 nm) as the reactivation light source. The results of these experiments are illustrated in Figure 5. All cases showed higher recoveries, during the repair phase, than the portion of cells restored during the dark repair. The maximum log recoveries of the dark- and photorepair experiments are shown in Table 2. During the repair phase and in the absence of DOM, recovery of UV_{254}-dosed *E. coli* was lower than that of the UV_{278}-dosing case. Net log recoveries were also calculated for the first 3 h of photorepair by taking the difference of the photorepair case and the observed decay of diluted *E. coli* under PRL1 which were not exposed to UVC; these values are shown in Table 3. The presence of CB increased the rate of photorepair after exposure to both wavelengths. Conversely, the addition of HA inhibited the initial photorepair after UV_{278}-dosing but did not change the UV_{254}-dosing case. After 3 h a decay phase was observed under PRL1, where UVA damage caused cell viability to decline. UVA is known to affect bacterial survivability by several mechanisms, including membrane damage,(46) photo-induced oxidative stress,(47-49) and decreased metabolic activity.(50) The decay rate constants for the experiments were estimated by linear regression from 3 h to 9 h, as

shown in Figure S3 and recorded in Table S1. Rates were not observed to be meaningfully different when compared across dosing wavelengths or DOM conditions. Notably, a correlation generated for all cases of decay post-photorepair (see Figure S3(b)), was different ($p < 0.05$) from the case where *E. coli* was exposed to UVA without prior UVC exposure. The non-repair case had a decay constant of 0.17 h^{-1}, while the collective decay constant for the photorepair cases was 0.33 h^{-1}. Despite the initial photoreactivation effect, *E. coli* were more susceptible to UVA irradiation after UVC-dosing.

Table 2. The mean and standard error recoveries ($\log[N/N_d]$) in the initial 3 h after UVC inactivation and for dark- and photorepair experiments.

Conditions	**UV_{254}-dosed**		**UV_{278}-dosed**	
	Dark Repair	Photoreactivation	Dark Repair	Photoreactivation
Without DOM	0.98 ± 0.04	1.96 ± 0.07	0.85 ± 0.1	2.50 ± 0.15
With HA	0.37 ± 0.09	2.03 ± 0.01	1.15 ± 0.07	1.94 ± 0.04
With CB	0.36 ± 0.05	3.20 ± 0.11	1.82 ± 0.04	3.13 ± 0.01

The photoreactivation profiles for all PRL1 cases comprised a repair phase in first 3 h followed by a decay period thereafter. This trend differed from photoreactivation described by Nebot Sanz et al. (2007) and Nyangaresi et al. (2018), which entailed growth, stationary, and mortality phases.(36, 51) While their models used a zeroth order decay constant for bacteria mortality, a first order decay was observed in the present study, induced by more intense UVA irradiation. The photoreactivation profiles observed here more closely match a model developed to predict solar reactivation of wastewater discharges, which incorporated a first order decay term.(27) The differences between models highlight the importance of reporting reactivation fluences and the consideration of the context where photorepair may occur. Figure 5(b) plots recoveries under PRL1 by fluence. The highest recovery observed occurred at ~65 J/cm^2, a value much higher than an estimated 1.44 J/cm^2 in the report by Nebot Sanz et al., based on their reported conditions of 4 h of 0.1 mW/cm^2 UVA. PRL1 provides a reasonable representation of intense

312 solar light, since typical solar UVA irradiance values reach upwards of 5.0 mW/cm^2, which
313 corresponds to 162 J/cm^2 over 9 h.(52)

314 **Table 3.** Repair (log[N/N$_d$]) during initial 3 h of photoreactivation after UV$_{254}$- or UV$_{278}$-
315 dosing, adjusted for observed growth or decay observations without UVC exposure. Error
316 values represent standard error.

Reactivation Condition	Log repair (UV$_{254}$-dosed)	Log repair (UV$_{278}$-dosed)
PRL1	2.20 ± 0.03	2.74 ± 0.05
PRL1 + HA	2.27 ± 0.01	2.18 ± 0.02
PRL1 + CB	3.44 ± 0.04	3.37 ± 0.01
PRL2	1.65 ± 0.01	2.30 ± 0.04
PRL3	1.36 ± 0.05	1.40 ± 0.04
PRL4	2.26 ± 0.07	2.16 ± 0.06
PRL5	1.82 ± 0.07	2.27 ± 0.03

317

318 *3.3.1. Effects of Photoreactivation Light Intensity*

319 Given the importance of reactivation light dose, experiments were performed using three
320 different intensities to disambiguate the roles of reactivation time and dose on the photorepair
321 process. Three UV$_{395}$ light sources were used to test the effects of photoreactivation intensities
322 on the photorepair process: PRL1 providing the highest intensity, followed by PRL2, then
323 PRL3. The spectra for the light sources are shown in Figure 2(a). Data from photoreactivation
324 experiments with these light conditions are displayed in Figure 6. After inactivation with UV$_{278}$
325 light, bacteria recovered at the same rate for PRL1 and PRL2 in the first 3 h, but the decay for
326 PRL2 was much slower than that for PRL1. The repair phase for recovery under PRL2 lasted
327 for just 3 h after UV$_{278}$-dosing, but after UV$_{254}$-dosing it lasted for 6 h. Reactivation under
328 PRL3, the least intense lamp, yielded recovery that extended to 6 h for the UV$_{278}$-dosed bacteria
329 and through 9 h for the UV$_{254}$ case. The log repair maxima under PRL2 and PRL3 were similar,
330 and both were lower than the PRL1 recovery. The UVA reactivation dose was important
331 because UVA is only sublethal up to about 40 J/cm^2 for stationary phase bacteria.(53, 54) After
332 this point, cellular repair and protection processes may have been overwhelmed by the stress of

the incident light. For example, UVA-sensitive chromophores within bacterial cells can cause thiouridine crosslinking, leading to depressed protein synthesis.(54)

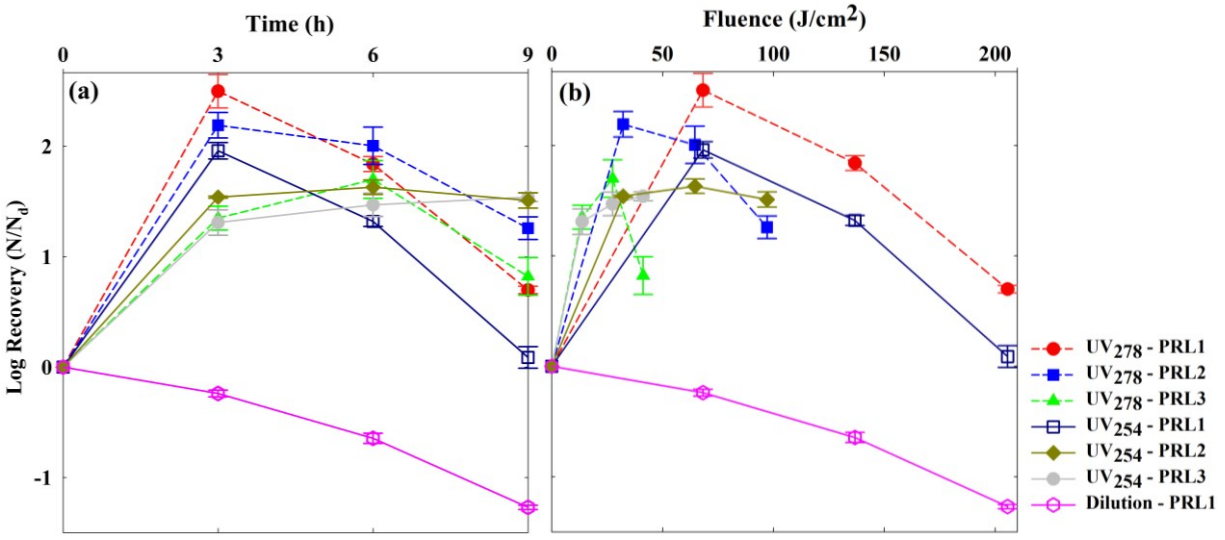

Figure 6. Photoreactivation of UV_{254}- or UV_{278}-dosed *E. coli* under different reactivation light intensities based on (a) time and (b) fluence. A reference of *E. coli* inactivation under PRL1 after dilution instead of UVC-dosing is also shown (—○—).

Variations in photoreactivation capacities, as measured by the lengths of photorepair phases, are likely affected by two factors: the reactivation dosage received and the type of damage inflicted during disinfection. In 2021 Pousty et al. confirmed that intracellular damage mechanisms depend on UV wavelength and showed that reactive oxygen species can damage DNA or cause general oxidative stress.(45) Photoreactivation trends for the three UV_{395} lamps, each with different intensities, are shown in Figure 6(b). Upon examination of the time and fluence reactivation profiles, one distinction is immediately apparent between UV_{254}- and UV_{278}-dosed cases. The peak recovery value for UV_{254}-dosed *E. coli* was reached at approximately 65 J/cm^2 regardless of light intensity (this fluence was only reached for PRL1 and PRL2 but PRL3's trend appears to be nearing a plateau before 50 J/cm^2). However, UV_{278}-dosed *E. coli* were subsequently less resistant to UV_{395} at low light intensities (PRL2 and PRL3). It is likely that oxidative stress introduced by UVA interferes with the photolyase repair pathway; a report by Song et al. in 2019 demonstrated that UVA pretreatment followed by UVC

dosing prevented subsequent photorepair.(55) From these data, it is clear that the photoreactivation process depends on both time and irradiation intensity; neither fluence- nor time-based calculations provide a complete understanding of the photoreactivation process. This observation demonstrates that at high fluences the reactivation model suggested by Bohrerova and Linden does not predict reactivation, just as they surmised in their analysis, because of a decay term.(56) The VC model provides a similar framework which uses a first order decay constant to account for damage by sunlight. All UVA photorepair experiments, except the UV_{254}-PRL2 and -PRL3 cases, appear to have a first order decay period after initial reactivation. The exceptions here would be better fit to a zero-order decay term as suggested by studies using low intensity reactivation lamps.(36, 51) The susceptibility of *E. coli* to UV_{395} depended on the wavelength of prior UVC exposure, and the rate of UVA-induced inactivation did not depend on fluence in a linear manner. This difference in cell susceptibilities shows that UV_{278}-dosing damaged *E. coli* in a different manner (likely oxidative stress) compared to UV_{254}.(45) A simple explanation would be that UV_{278}-dosing damages cellular mechanisms that provide UVA resistance. An alternate hypothesis is that *E. coli* can recover more quickly from UV_{278}-dosing, leading to a higher repair rate—an observation borne out in nearly all experiments here. Rapid growth rates make bacteria more vulnerable to stressors like heat or UVA,(53) but it is not clear if this principle would apply to regrowth from repair processes in the same manner. Further investigation is needed to identify the mechanisms responsible for the differential behavior of UV_{254}- and UV_{278}-dosed *E. coli*.

3.3.2. Effects of Photoreactivation Wavelength

Light sources of different wavelengths were applied for the photoreactivation to assess the effects of the photon energy on the photorepair process; emission spectra of these light sources are illustrated in Figure 2(b). The results of photoreactivation under different wavelengths, on a time basis, are shown in Figure 7(a). Photorepair was observed in the first three hours in all

cases. In contrast to the other PRLs, photoreactivation under the visible light (PRL5) maintained continued throughout the 9 h, undergoing some growth in addition to repair. The rate of photorepair under exposure of 365 nm light (PRL4), on the other hand, was lower than both PRL1 and PRL5. PRL4 induced the most decay after the recovery phase among all light sources and based on the work of Nelson et al. (2018), UV_{365} causes damage through the production

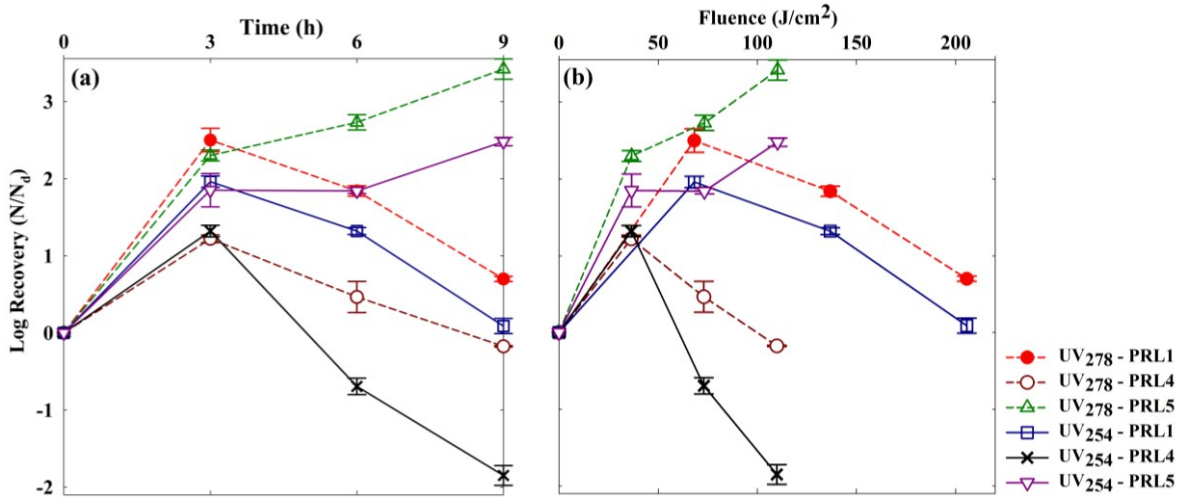

Figure 7. Photoreactivation of *E. coli* using different light sources after inactivation with UV_{254} and UV_{278} based on (a) time and (b) fluence.

of reactive oxygen species or photochemically produced reactive intermediates,(29) explaining the higher inactivation compared to other PRLs. Inactivation kinetics under these conditions without prior disinfection are shown in Figure S4, and the inactivation values at 3 h were used to calculate the log repair values provided in Table 3. In general, recovery in the UV_{278}-dosed cases were higher than the UV_{254}-dosed cases. The pattern for photoreactivation with PRL4 was the same as PRL1: a repair phase followed by an inactivation phase.

The fluence-basis data for photorepair under various reactivation light spectra are plotted in Figure 7(b). Little difference was observed between the fluence- and time- bases for the disparate lights. Both time-based and fluence-based calculations confirmed that the amount of photoreactivation under visible light was higher than under UV_{395} or UV_{365}. Although Bohrerova and Linden reported that there was no significant change in photorepair rate between several visible lamp types (full spectrum lamps (5500K), cool white lamps (2700K), and

fluorescent lamps (5500K)),(56) differences between UVA light sources are certainly important, due to lethal effects at high fluences. A cell's ability to perform photorepair depends on three factors: the presence of photolyase in the cell, the number of photons received, and the wavelength of the light.(57) The larger maximum log recoveries found for the visible light cases may be explained by the enzyme's light absorption, which is strongest in the visible range,(19, 54) but the situation is complicated by deleterious effects of UVA. The differential effects of photoreactivation wavelengths were described by Jagger (1981), in which he reported that sublethal effects could be observed up to a specific, wavelength-dependent dose limit. Specifically, the sublethal effects were found to begin at about 2 J/cm^2 for UV_{334} and 10 J/cm^2 for UV_{366}, reaching lethality at roughly one order of magnitude higher fluence.(58) Sublethal effects might have also contributed to the slowing initial repair in the UVA cases compared to visible, but this effect was small compared to the result of reaching lethal UVA doses. In parallel to the observed trend for the high intensity UV_{395} lamp (PRL1, Figure 6), the decay phase during photoreactivation by UV_{365} was more pronounced after disinfection by UV_{254} than with UV_{278}.

3.3.3. Photoreactivation Model Fitting

The rate constants for reactivation and decay by UVA during photoreactivation were estimated by employing the VC model fitted to experimental data with additional timepoints before 3 h. Figure 8 shows survival fractions UV_{254}- or UV_{278}-dosed of *E. coli* during photoreactivation under PRL1 compared to predicted trends from either VC model parameter estimations,(27) using 13.75 mJ/cm^2 as the UV_{254} fluence value, or based on a non-linear regression of the observed data. Even though the same *E. coli* strain (ATCC 15597) was used in both studies, a direct comparison was not appropriate due to differences in inactivation and photoreactivation light wavelengths and fluences. In their work, Velez-Colmenares and coworkers (2012) derived empirical relationships between several parameters (S_m, k_s, and $[S_m - S_o]$) and UV_{254} fluence, from 50 to 150 mJ/cm^2. While it is not clear that they accounted for light attenuation or other

415 factors within their reactor, the 13.75 mJ/cm^2 UV_{254} applied here requires unreasonable
416 extrapolation. The VC model used an M_s value derived from the solar decay of *E. coli*, whereas
417 PRL1 is a high intensity UV_{395} source.(27) For these reasons, it is not surprising that the
418 fluence-based parameter estimates did not fit the UV_{254} observations here. Using a non-linear
419 regression to fit the observed data, however, yielded good fits for both UV_{254} and UV_{278}
420 photoreactivation profiles, with R^2 coefficients of 0.967 and 0.979, respectively.

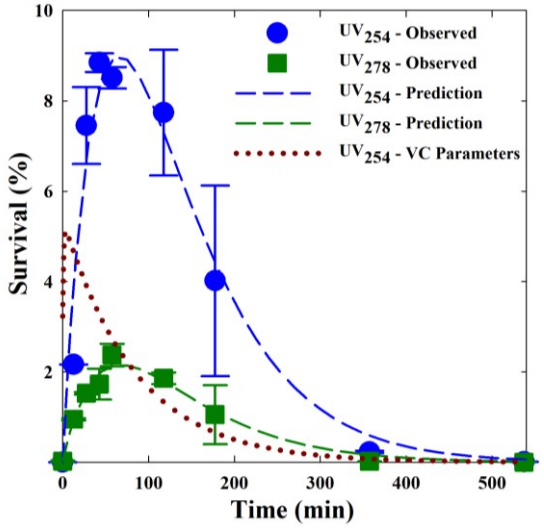

Figure 8. Observed survival fractions during photoreactivation of UV_{254}- and UV_{278}-dosed *E. coli* with corresponding non-linear fits and a UV_{254} prediction using parameters from the Velez-Colmenares formulae.

421

422 The estimated and regression-fitted parameters are tabulated in Table 4. The M_s values derived
423 here (0.0136 and 0.0132 min^{-1}) were close to 0.0119 min^{-1} used by Velez-Colmenares et al.
424 (2018). These decay constants are significantly larger, however, than the decay rate observed
425 under PRL1 (0.00283 min^{-1}) with no prior UVC irradiation, indicating that UVC dosing causes
426 *E. coli* to be more susceptible to subsequent UVA exposure. Differences in S_m and k_s values
427 were most notable compared to the previous report,**(27)** both likely explained by the disparate
428 experimental conditions described above. The fitted parameters, then, provide more reasonable
429 values. Here, a high S_m indicates that many, if not all, of the damaged cells can be repaired after
430 UV_{254} or UV_{278} doses that caused initial 3-log reductions to viability. Conversely, the observed

k_s values were much smaller than those reported in Velez-Colmenares et al. (2012); the small fraction of repairable bacteria in their work, due to large inactivation doses, inflates k_s compared to cases where the majority of bacteria can undergo photorepair. The peak recoveries observed here occurred between 60 and 75 minutes under PRL1, whereas the 2012 study showed peak reactivation within the first 10 minutes of photorepair.**(27)** Notably, the UV_{254} dosed bacteria recovered to a much higher fraction than UV_{278} upon examination of data points within the first two hours of reactivation. The slower repair kinetics observed here have significant environmental implications, because fecal coliform monitoring in wastewater effluent will not provide accurate estimates of the discharge's real impact if photorepair causes peak recovery downstream. Considering the DOM (Figure 5) and reactivation wavelength experiments (Figures 6 and 7), it is apparent that the delayed recovery maxima are exacerbated by two factors. First, nutritious DOM increases the effective S_m by allowing growth in addition to repair. Second, variations in reactivation light intensity and wavelength can change M_s and k_s. Prediction of the time at which maximum recoveries occur may be as important, if not more so, than the maximum values.

Table 4. Model parameters, calculated or fitted, used in the predictive models for survival in Figure 8, with corresponding R^2 values.

Parameter	Calculated UV_{254}[a]	Fitted UV_{254}	Fitted UV_{278}
S_m	5.41	104.7	27.5
M_s	0.0119	0.0136	0.0132
k_s	1.03	0.00358	0.00313
$(S_m - S_o)$	2.18	104.7	27.5
R^2	N/A	0.967	0.979

[a]Values taken from or calculated according to empirical formulae by Velez-Colmenares et al. (2012).

4. Conclusions

The examination of photoreactivation conditions revealed three important considerations regarding UV disinfection applications. First, according to *E. coli* survival fractions and

susceptibilities to low intensity UVA, UV_{278}-dosing may yield a net, comparative benefit in inactivation credit for wastewater discharges into waters receiving moderate to low amounts of sunlight. On the other hand, a red-shift in disinfection wavelengths appeared to increase the recovery potential for *E. coli* in the dark, especially in the presence of plentiful nutrients. These contrasting effects reveal a significant need to better understand and model systems where both dark and photorepair processes are expected to occur in tandem (e.g. wastewater discharged to a murky column of water with limited UV light penetration). Second, new challenges to the development of predictive models of photoreactivation were identified. If photoreactivation was dependent solely on the absorption of photons by photolyase, then reactivation fluence would predict the photorepair dynamics. The results here, however, point to the combined relevance of time and light intensity on the repair rate and to the dependence of UVA-induced decay on the reactivation light intensity and wavelength. Further study is required to establish empirical relationships between these factors and their corresponding model parameters (i.e., M_s and k_s). In addition to the influence of reactivation parameters, the results here also point to a need for improved parameterization on the UVC dosing side of the system.

Finally, established empirical relationships for model parameters were unable to predict observations here, despite using the same *E. coli* strain and UV_{254}. The VC model and the associated parameterizations were based on pilot dosing systems which undoubtedly functioned as a non-ideal reactor,(27) whereas the present study—like many others—used small batch reactors to approximate ideal mixing conditions. This difference evokes an important question of how to properly account for a distribution of dosages which will inevitably result in non-ideal reactor conditions when predicting reactivation profiles. There is a critical need to define and measure UV dosing in terms of fluence experienced by the treated water rather than on the basis of lamp outputs. The translation of laboratory studies to full scale treatment facilities is vital but currently insufficient; future models should incorporate a distribution of UV-dosages

received by bacteria as occurs in non-ideal systems. Some regulatory estimations exist for accounting for the repair of bacteria in wastewater effluent and operational conditions can be adjusted to mitigate photorepair,(59) but these efforts are currently rudimentary in nature and require improvements in order to effectively account for variable conditions and novel disinfection wavelengths. Current predictive models and their parameterization must be improved to empower regulators and practitioners to better manage wastewater discharges and adapt to new UV technologies.

Acknowledgments

This work was supported by the Louisiana Board of Regents Research Competitiveness Subprogram grant # LEQSF(2017-20)-RD-A-06 and by the National Science Foundation under awards 1952409 and 2046660.

References

1. Prüss A, Kay D, Fewtrell L, Bartram J. Estimating the burden of disease from water, sanitation, and hygiene at a global level. Environ Health Perspect. 2002;110(5):537-42.
2. Ashbolt NJ. Microbial Contamination of Drinking Water and Human Health from Community Water Systems. Curr Environ Health Rep. 2015;2(1):95-106.
3. Hijnen WAM, Beerendonk EF, Medema GJ. Inactivation credit of UV radiation for viruses, bacteria and protozoan (oo)cysts in water: A review. Water Res. 2006;40(1):3-22.
4. Rodriguez RA, Bounty S, Beck S, Chan C, McGuire C, Linden KG. Photoreactivation of bacteriophages after UV disinfection: Role of genome structure and impacts of UV source. Water Res. 2014;55:143-9.
5. Würtele MA, Kolbe T, Lipsz M, Külberg A, Weyers M, Kneissl M, et al. Application of GaN-based ultraviolet-C light emitting diodes – UV LEDs – for water disinfection. Water Res. 2011;45(3):1481-9.
6. Bolton James R, Cotton Christine A. Ultraviolet Disinfection Handbook. 1st ed. Denver: American Water Works Association (AWWA); 2011.
7. Vilhunen S, Särkkä H, Sillanpää M. Ultraviolet light-emitting diodes in water disinfection. Environmental Science and Pollution Research. 2009;16(4):439-42.
8. Banas MA, Crawford MH, Ruby DS, Ross MP, Nelson JS, Allerman AA, et al. Final LDRD report: ultraviolet water purification systems for rural environments and mobile applications. Sandia National Laboratories; 2005.
9. Hu X, Deng J, Zhang JP, Lunev A, Bilenko Y, Katona T, et al. Deep ultraviolet light-emitting diodes. physica status solidi (a). 2006;203(7):1815-8.
10. Song K, Mohseni M, Taghipour F. Application of ultraviolet light-emitting diodes (UV-LEDs) for water disinfection: A review. Water Res. 2016;94:341-9.
11. Harris TR, Pagan JG, Batoni P. Optical and Fluidic Co-Design of a UV-LED Water Disinfection Chamber. ECS Transactions. 2013;45(17):11-8.

12. Standard AN. Ultraviolet Microbiological Water Treatment Systems. NSF/ANSI 55. USA: NSF International; 2019.
13. Chatterjee N, Walker GC. Mechanisms of DNA damage, repair, and mutagenesis. Environmental and Molecular Mutagenesis. 2017;58(5):235-63.
14. Sinha RP, Häder D-P. UV-induced DNA damage and repair: a review. Photochemical & Photobiological Sciences. 2002;1(4):225-36.
15. Jungfer C, Schwartz T, Obst U. UV-induced dark repair mechanisms in bacteria associated with drinking water. Water Res. 2007;41(1):188-96.
16. Smith KC, Wang T-CV, Sharma RC. recA-Dependent DNA repair in UV-irradiated Escherichia coli. Journal of Photochemistry and Photobiology B: Biology. 1987;1(1):1-11.
17. Setlow RB, Carrier WL. The Disappearance of Thymine Dimers from DNA: An Error-Correcting Mechanism. Proc Natl Acad Sci U S A. 1964;51(2):226-31.
18. Jagger J. Photoreactivation. Bacteriol Rev. 1958;22(2):99-142.
19. Sancar A. Structure and Function of DNA Photolyase and Cryptochrome Blue-Light Photoreceptors. Chemical Reviews. 2003;103(6):2203-38.
20. Marizcurrena JJ, Martínez-López W, Ma H, Lamparter T, Castro-Sowinski S. A highly efficient and cost-effective recombinant production of a bacterial photolyase from the Antarctic isolate Hymenobacter sp. UV11. Extremophiles. 2019;23(1):49-57.
21. Gaston KJ, Bennie J, Davies TW, Hopkins J. The ecological impacts of nighttime light pollution: a mechanistic appraisal. Biological Reviews of the Cambridge Philosophical Society. 2013;88(4):912-27.
22. Song K, Taghipour F, Mohseni M. Microorganisms inactivation by wavelength combinations of ultraviolet light-emitting diodes (UV-LEDs). Science of The Total Environment. 2019;665:1103-10.
23. Kashimada K, Kamiko N, Yamamoto K, Ohgaki S. Assessment of photoreactivation following ultraviolet light disinfection. Water Science and Technology. 1996;33(10):261-9.
24. Tosa K, Hirata T. Photoreactivation of enterohemorrhagic Escherichia coli following UV disinfection. Water Res. 1999;33(2):361-6.
25. Beggs CB. A quantitative method for evaluating the photoreactivation of ultraviolet damaged microorganisms. Photochemical & Photobiological Sciences. 2002;1(6):431-7.
26. Sahan M. The measurements of the global solar radiation and solar ultraviolet radiation during 2018 year. AIP Conference Proceedings. 2019;2178(1):030016.
27. Velez-Colmenares JJ, Acevedo A, Salcedo I, Nebot E. New kinetic model for predicting the photoreactivation of bacteria with sunlight. J Photochem Photobiol B-Biol. 2012;117:278-85.
28. Chan H-L, Gaffney PR, Waterfield MD, Anderle H, Peter Matthiessen H, Schwarz H-P, et al. Proteomic analysis of UVC irradiation-induced damage of plasma proteins: Serum amyloid P component as a major target of photolysis. FEBS Letters. 2006;580(13):3229-36.
29. Nelson KL, Boehm AB, Davies-Colley RJ, Dodd MC, Kohn T, Linden KG, et al. Sunlight-mediated inactivation of health-relevant microorganisms in water: a review of mechanisms and modeling approaches. Environmental Science: Processes & Impacts. 2018;20(8):1089-122.
30. Li G-Q, Wang W-L, Huo Z-Y, Lu Y, Hu H-Y. Comparison of UV-LED and low pressure UV for water disinfection: Photoreactivation and dark repair of Escherichia coli. Water Res. 2017;126:134-43.
31. Thiagarajan V, Byrdin M, Eker APM, Müller P, Brettel K. Kinetics of cyclobutane thymine dimer splitting by DNA photolyase directly monitored in the UV. Proc Natl Acad Sci U S A. 2011;108(23):9402-7.
32. Douki T, Sage E. Dewar valence isomers, the third type of environmentally relevant DNA photoproducts induced by solar radiation. Photochemical & Photobiological Sciences. 2016;15(1):24-30.
33. Foukal P. Solar astrophysics. . 2nd ed: Wiley-VCH; 2004.
34. Kollu K, Ormeci B. Regrowth Potential of Bacteria after Ultraviolet Disinfection in the Absence of Light and Dark Repair. Journal of Environmental Engineering. 2015;141(3).
35. Thomas JD. The role of dissolved organic matter, particularly free amino acids and humic substances, in freshwater ecosystems. Freshwater Biology. 1997;38(1):1-36.

36. Nyangaresi PO, Qin Y, Chen G, Zhang B, Lu Y, Shen L. Effects of single and combined UV-LEDs on inactivation and subsequent reactivation of E. coli in water disinfection. Water Res. 2018;147:331-41.
37. Cormier J, Janes M. A double layer plaque assay using spread plate technique for enumeration of bacteriophage MS2. J Virol Methods. 2014;196:86-92.
38. Bolton JR, Linden KG. Standardization of Methods for Fluence (UV Dose) Determination in Bench-Scale UV Experiments. Journal of Environmental Engineering. 2003;129(3):209-15.
39. Murov SL, Hug GL, Carmichael I. Handbook of photochemistry. 2nd ed., rev. and expanded. ed: M. Dekker; 1993.
40. Beck SE, Ryu H, Boczek LA, Cashdollar JL, Jeanis KM, Rosenblum JS, et al. Evaluating UV-C LED disinfection performance and investigating potential dual-wavelength synergy. Water Res. 2017;109:207-16.
41. Muela A, Garcia-Bringas JM, Arana I, Barcina I. Humic Materials Offer Photoprotective Effect to Escherichia coli Exposed to Damaging Luminous Radiation. Microbial Ecology. 2000;40(4):336-44.
42. Tikhonov VV, Yakushev AV, Zavgorodnyaya YA, Byzov BA, Demin VV. Effects of humic acids on the growth of bacteria. Eurasian Soil Science. 2010;43(3):305-13.
43. Bren A, Park JO, Towbin BD, Dekel E, Rabinowitz JD, Alon U. Glucose becomes one of the worst carbon sources for E.coli on poor nitrogen sources due to suboptimal levels of cAMP. Sci Rep. 2016;6:24834-.
44. Besaratinia A, Yoon JI, Schroeder C, Bradforth SE, Cockburn M, Pfeifer GP. Wavelength dependence of ultraviolet radiation-induced DNA damage as determined by laser irradiation suggests that cyclobutane pyrimidine dimers are the principal DNA lesions produced by terrestrial sunlight. FASEB J. 2011;25(9):3079-91.
45. Pousty D, Hofmann R, Gerchman Y, Mamane H. Wavelength-dependent time–dose reciprocity and stress mechanism for UV-LED disinfection of Escherichia coli. Journal of Photochemistry and Photobiology B: Biology. 2021;217:112129.
46. Hoerter JD, Arnold AA, Kuczynska DA, Shibuya A, Ward CS, Sauer MG, et al. Effects of sublethal UVA irradiation on activity levels of oxidative defense enzymes and protein oxidation in Escherichia coli. Journal of Photochemistry and Photobiology B: Biology. 2005;81(3):171-80.
47. Bosshard F, Riedel K, Schneider T, Geiser C, Bucheli M, Egli T. Protein oxidation and aggregation in UVA-irradiated Escherichia coli cells as signs of accelerated cellular senescence. Environmental Microbiology. 2010;12(11):2931-45.
48. Cadet J, Sage E, Douki T. Ultraviolet radiation-mediated damage to cellular DNA. Mutation Research, Fundamental and Molecular Mechanisms of Mutagenesis. 2005;571(1):3-17.
49. Anesio AM, Granéli W, Aiken GR, Kieber DJ, Mopper K. Effect of Humic Substance Photodegradation on Bacterial Growth and Respiration in Lake Water. Appl Environ Microbiol. 2005;71(10):6267-75.
50. Bosshard F, Bucheli M, Meur Y, Egli T. The respiratory chain is the cell's Achilles' heel during UVA inactivation in Escherichia coli. Microbiology. 2010;156(7):2006-15.
51. Nebot Sanz E, Salcedo Dávila I, Andrade Balao JA, Quiroga Alonso JM. Modelling of reactivation after UV disinfection: Effect of UV-C dose on subsequent photoreactivation and dark repair. Water Res. 2007;41(14):3141-51.
52. Roshan DR, Koc M, Abdallah A, Martin-Pomares L, Isaifan R, Fountoukis C. UV Index Forecasting under the Influence of Desert Dust: Evaluation against Surface and Satellite-Retrieved Data. Atmosphere. 2020;11(1):17.
53. Berney M, Weilenmann HU, Ihssen J, Bassin C, Egli T. Specific growth rate determines the sensitivity of Escherichia coli to thermal, UVA, and solar disinfection. Appl Environ Microbiol. 2006;72(4):2586-93.
54. Probst-Rüd S, McNeill K, Ackermann M. Thiouridine residues in tRNAs are responsible for a synergistic effect of UVA and UVB light in photoinactivation of Escherichia coli. Environmental Microbiology. 2017;19(2):434-42.

619 55. Song K, Mohseni M, Taghipour F. Mechanisms investigation on bacterial inactivation through
620 combinations of UV wavelengths. Water Res. 2019;163:9.
621 56. Bohrerova Z, Linden KG. Standardizing photoreactivation: Comparison of DNA photorepair rate
622 in Escherichia coli using four different fluorescent lamps. Water Res. 2007;41(12):2832-8.
623 57. Gayán E, Condón S, Álvarez I. Biological Aspects in Food Preservation by Ultraviolet Light: a
624 Review. Food and Bioprocess Technology. 2014;7(1):1-20.
625 58. Jagger J. Near-UV radiation effects on microorganisms. Photochemistry and Photobiology.
626 1981;34(6):761-8.
627 59. Hallmich C, Gehr R. Effect of pre- and post-UV disinfection conditions on photoreactivation of
628 fecal coliforms in wastewater effluents. Water Res. 2010;44(9):2885-93.
629